

## Claremont Colleges Scholarship @ Claremont

---

WM Keck Science Faculty Papers

W.M. Keck Science Department

---

4-16-2001

# Large-Scale Synchrony in Weakly Interacting Automata

Eric J. Friedman  
*Cornell University*

Adam S. Landsberg  
*Claremont McKenna College; Pitzer College; Scripps College*

---

### Recommended Citation

Friedman, E.J., and A.S. Landsberg. "Large-Scale Synchrony in Weakly Interacting Automata." *Physical Review E* 63.5 (2001): 51303.  
DOI: 10.1103/PhysRevE.63.051303

This Article is brought to you for free and open access by the W.M. Keck Science Department at Scholarship @ Claremont. It has been accepted for inclusion in WM Keck Science Faculty Papers by an authorized administrator of Scholarship @ Claremont. For more information, please contact [scholarship@cuc.claremont.edu](mailto:scholarship@cuc.claremont.edu).

## Large-scale synchrony in weakly interacting automata

Eric J. Friedman<sup>1</sup> and A. S. Landsberg<sup>2</sup><sup>1</sup>*Department of Economics, Rutgers University, New Brunswick, New Jersey 08903*<sup>2</sup>*W. M. Keck Science Center, The Claremont Colleges, Claremont, California 91711*

(Received 8 December 2000; published 16 April 2001)

We study the behavior of two spatially distributed (sandpile) models which are weakly linked with one another. Using a Monte Carlo implementation of the renormalization-group and algebraic methods, we describe how large-scale correlations emerge between the two systems, leading to synchronized behavior.

DOI: 10.1103/PhysRevE.63.051303

PACS number(s): 45.70.Ht, 64.60.Ak, 05.45.Xt, 05.65.+b

### I. INTRODUCTION

Interacting systems have long been the subject of considerable interest and study, and they can display a rich variety of behaviors. One of the premier concepts that has emerged from such studies is the notion of synchronization, both in its traditional sense as well as in one of its modern variants (e.g., phase synchronization, lag synchronization, etc.) [1–4]. A particularly interesting class of systems to consider in light of these broadening notions of synchronization is provided by automata (“sandpile”) models. Automata offer a rich assortment of well-studied, complex behaviors (e.g., self-organized criticality [5]), and have been used extensively in the literature to model a variety of physical phenomena (e.g., [6]). If two such automata are permitted to weakly interact [7], an interesting type of synchronization effect is seen to emerge: While small events on one sandpile are essentially uncorrelated with small events on the other, large-scale events are so highly correlated that not only is a large event on one sandpile almost always concomitant with a large event on the other sandpile, but the two events are in fact approximately equal in magnitude (with rms fractional deviation approaching zero) (see Fig. 1). This result holds despite the weakness of the coupling between the sandpiles. Note that this “synchronization” between sandpiles is not periodic (i.e., the time interval between synchronized large-scale events is not fixed), nor is it completely random (since correlations exist between temporal spacing of events and event size.)

We can glean some basic insight into the origin of this form of synchronization from a relatively simple plausibility argument: As a large avalanche sweeps across one sandpile, it will, owing to the weak coupling, spill some small yet nontrivial number of grains onto the other sandpile. Since sandpile models (like other self-organized critical systems) are capable of generating avalanches of all sizes, these spilled grains could conceivably induce a large subsidiary avalanche in the second sandpile. In turn, this subsidiary avalanche could spill some grains back onto the first sandpile, and so on. In this manner, it is possible to imagine how high levels of correlations might develop between the two sandpiles during large events. It is thus reasonable to conjecture that through such feedback and mutual reinforcement, a large avalanche starting on one sandpile would have a very high probability of inducing a (simultaneous) avalanche of comparable magnitude on the other sandpile, despite the

weakness of the coupling. Indeed, from this scenario one might also infer that perhaps these avalanches would not merely be comparable in size, but in fact nearly *equal* in size (that this should be the case is certainly plausible, though, admittedly, not compelling).

While this intuitive argument is helpful, understanding the actual process by which intersandpile correlations develop proves to be surprisingly subtle and interesting. The purpose of this paper is to examine the nature of this complex interplay between interacting automata, and to show how it produces the observed large-scale synchronous behavior. To do so, we use a modification of a renormalization-group procedure originally developed by Refs. [8–10] for single-sandpile models, along with an algebraic technique. Our renormalization procedure, in fact, turns out to be interesting in its own right, since it is implemented using a Monte Carlo method which proves to be highly efficient, thus rendering previously intractable renormalization calculations easily computable. As a result, the methodology we employ here is likely to be applicable to a variety of related automata problems. This paper is organized as follows. In Sec. II we present a prototype interacting-sandpile model and describe numerical simulations which demonstrate the emergence of large-scale synchrony. Section III contains a detailed discussion of the renormalization procedure itself and its predictions. We also describe an alternative algebraic approach which proves useful for understanding certain key features of the model, including the appearance of so-called “coupling symmetry.” Generalizations of the basic model are also described.

### II. BASIC MODEL AND PHENOMENOLOGY

To begin, we recall a classic sandpile model studied by Dhar and Ramaswamy [11]. The system consists of a two-dimensional square lattice, where to each lattice site  $ij$  one ascribes a non-negative integer  $h(i,j)$ . The function  $h(i,j)$  is called the “height” and represents the number of “sandgrains” on a given site. The system evolves as follows: A lattice site is selected at random, and one grain is added to that site. Provided the new height does not exceed a certain critical value (taken throughout this paper to be 4), then nothing further happens. If, however, the critical height is exceeded, then that site will “topple” [ $h(i,j) \rightarrow h(i,j) - 2$ ] and spill one grain to its neighbor on the right [ $h(i,j+1) \rightarrow h(i,j+1) + 1$ ] and one to its neighbor above

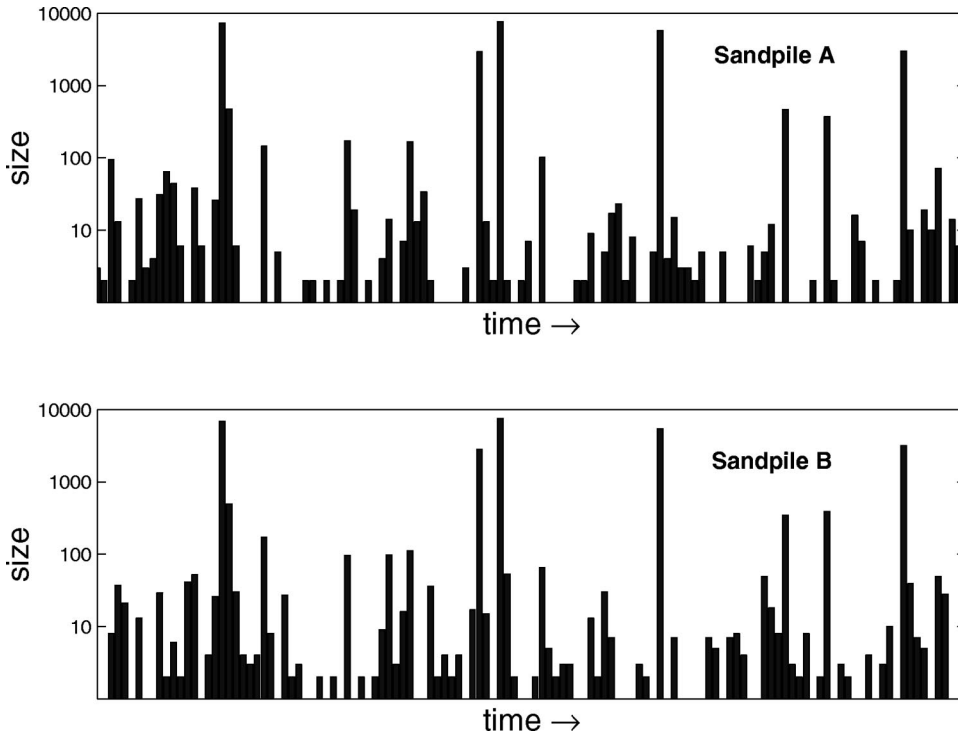


FIG. 1. A representative time series. Shown is the total number of topples on each sandpile for each in a series of avalanches. Note that large peaks occur simultaneously and are approximately equal in magnitude, while smaller peaks are relatively uncorrelated in both time and size. (The data set was generated from an automata model described in Sec. II. Note that for illustrative purposes, we have added one to the avalanche sizes in order to avoid singularities associated with the logarithmic scaling in the plots.)

$[h(i-1,j) \rightarrow h(i-1,j)+1]$ . The affected sites on the right and above may in turn topple (if their heights are above the critical threshold), and so on. In this manner, it is possible for an avalanche to spread across the lattice. This type of model is referred to as a “directed” sandpile, since an avalanche can only propagate upwards or to the right. Once an avalanche has exhausted itself, a new grain is dropped onto a randomly selected site (from either sandpile), and the process repeats. (We mention here that the asymptotic behavior of this model remains unchanged under a wide choice of dropping rules, as analyzed in Ref. [11].) The dynamics of this model (which is representative of a large class of related automaton models) is surprisingly complex and has been well documented [11,10]. One of its key features is that it exhibits avalanches of all sizes, where “size” refers to the total number of lattice sites that topple upon the addition of a single grain to the system.

Now consider a system of two (independent) directed sandpile models, each evolving according to the rules outlined above. The two sandpiles are assumed to be of identical dimension, so that for every lattice site on the first, one can associate a corresponding lattice site on the second. (Visually, we imagine two planar lattices, one atop the other. Each site on the top sheet is matched with the site immediately below.) We shall refer to these two lattices as “sheet A” and “sheet B,” respectively. We now allow the two sheets to interact according to the following rule: If a site on a given sheet topples, it will, as before, always spill two grains onto its own sheet (one to each of its neighboring sites on the right and above). Now, however, we assume this toppling site also has some nonzero probability  $\rho$  of spilling an additional two grains onto the other sheet (one to each of the neighboring sites on the right and above). In this latter case we require  $h(i,j;s) \rightarrow h(i,j;s)-4$ , where  $s$  denotes the sheet

on which the toppling site lies, so that sand is “conserved.” (Since this model is directed, it does not matter if the updating rules for the lattice are implemented sequentially or in parallel.) Note that when  $\rho=0$ , the two sheets are dynamically independent. Our study focuses on the weak-coupling regime ( $\rho \ll 1$ ). We shall henceforth refer to this particular model as the “two-sheet model” (generalizations will be described later).

In a series of numerical simulations on this coupled system, we added grains (one at a time) to randomly selected sites (on either sheet), and monitored the resulting avalanches. (Most simulations were carried out for  $L=1000$  and very few avalanches in the simulations reached the edge, so we expect edge effects to be minimal.) For each avalanche, we tracked the number of sites that toppled in each of the two sheets ( $N_A, N_B$ ), explicitly counting multiplicities if a given site underwent multiple topples. A representative graph is shown in Fig. 2. The high density of datapoints along the  $x$  and  $y$  axes of Fig. 2 for small avalanche sizes indicates that these small avalanches remain largely confined to the sheet on which they started; only rarely will they spill over to the other sheet. This is not surprising, since the two sheets are only very weakly coupled to one another ( $\rho=0.05$ ) and thus the dynamics on each can be expected to be essentially independent. However, for large avalanches, a new trend is clearly seen to emerge: Even though, at each individual lattice site, the probability of a grain spilling over to the other sheet remains very low, nonetheless a large avalanche starting on one sheet is seen to have an *equally* large effect on the other sheet. In particular, the total number of sites that topple on each sheet (in a given avalanche) become nearly equal in magnitude (Fig. 2), with a root-mean-square fractional deviation that approaches zero (Fig. 3, solid line). Qualitatively, it is as though the effective coupling strength

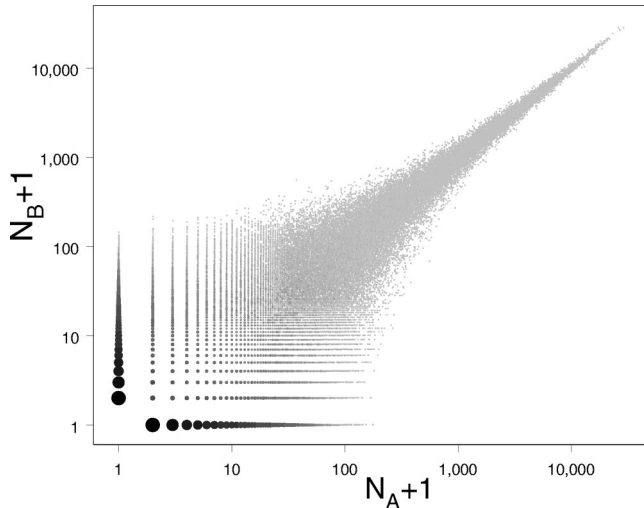


FIG. 2. Large-scale synchrony. The number of topples on each sheet during avalanches in the two-sheet model with coupling parameter  $\rho=0.05$  is shown. Observe that for large avalanche sizes strong correlations develop, with  $N_A$  and  $N_B$  becoming approximately equal.

between the two sheets increases with spatial scale (we will return to this point later). We note here (for emphasis) that had we included in Fig. 2 only those avalanches that were touched off by the addition of grains to, say, sheet A only, then the prominent trend towards the diagonal seen in the figure for large avalanche size would be unaffected.

Our goal is to show how this type of ‘‘large-scale synchrony’’ (LSS for short) arises between two such weakly

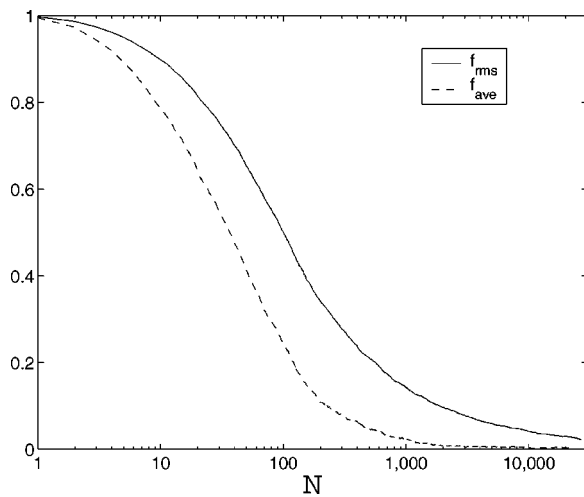


FIG. 3. The root-mean-square fractional deviation  $f_{rms}$  (solid line) between  $N_A$  and  $N_B$  vs avalanche size ( $N=N_A+N_B$ ) for the data shown in Fig. 2. The decrease in  $f_{rms}$  with size indicates that, on large length scales, the two sheets behave as though they were strongly coupled. A related phenomenon, ‘‘coupling symmetry’’ (see text), is illustrated by the dashed curve showing the average fractional deviation [ $f_{ave} = \langle (N_A - N_B) / (N_A + N_B) \rangle$ ], where the average is computed over only those avalanches that were initiated by the addition of one grain to sheet A. Observe that such avalanches, if small, remain primarily confined to sheet A (as expected), while large ones divide equally between the two sheets (since  $f_{ave} \rightarrow 0$ ).

interacting systems. We mention here that LSS also appears in a larger class of models than just the numerical example described above. For instance, one can construct ‘‘generalized two-sheet models,’’ in which sites are allowed to spill either one or two grains onto neighboring sites on either/both sheets according to some probability matrix. As we will show later, these generalized systems (subject to some mild restrictions, namely, an overall right/above symmetry) fall into the same universality class as our original two-sheet model and hence also exhibit LSS. (We have, in fact, found that power-law behavior—which is a characteristic of all the sandpile models to be discussed in this paper—is indeed not essential for the appearance of LSS).

### III. RENORMALIZATION-GROUP ANALYSIS

The fundamental behavior of these weakly interacting automata can be understood using a renormalization-group analysis, as we now describe. We base our work on the renormalization procedure developed by Hasty and Wiesenfeld [10] for (single sheet) directed-sandpile models, which extended key work by Pietronero and co-workers [8,9]. Adapting this procedure for systems of interacting automata, we show how it can be used to explain the emergence of LSS.

The basic idea behind the renormalization method is to repeatedly coarse grain the automaton lattice into cells of successively larger sizes. In our model, this means grouping the lattice sites on each sheet into  $2 \times 2$  blocks, then  $4 \times 4$  blocks, then  $8 \times 8$ , and so on. At each stage, dynamical evolution rules are constructed which describe the behavior of the cells. Each time the basic cell size is increased, new dynamical evolution rules are constructed. The so-called ‘‘RG map’’ is a mapping that links the evolution rules for these different cell sizes. The behavior of the original automaton model on large spatial scales can then be deduced by examining the limiting behavior (i.e., fixed points) of this RG map. Before proceeding, we remark here upon an important distinction between the coarse-graining procedure used here for our two-automata model and the procedure used for single-sheet models, as described by Refs. [10] and [8]. Specifically, because we are interested in how each sheet behaves individually, we do the coarse graining on each sheet individually, rather than following the standard procedure which would naturally treat the full two-sheet lattice as a single entity and coarse grain it into cells which span both sheets. (If this latter procedure is followed, one finds that under the RG mapping, the two-sheet model converges to the single-sheet model of Refs. [10] and [11], proving that the two models have the same critical exponent [12]. Unfortunately, all information regarding correlations between the two sheets is lost.)

In our model, the procedure works as follows. Imagine that the sites on sheets A and B have already been coarse grained  $n$  times, so that the individual sheets are divided up into large ‘‘cells,’’ each comprised of  $2^n \times 2^n$  individual lattice sites. Adapting the renormalization scheme of Refs. [8–10] to our system, the evolution rules for a cell can be expressed in terms of a  $3 \times 3$  probability matrix  $P^n$ . In par-

ticular, if a grain is added to a cell on a particular sheet, then the associated probability matrix is  $P^n = \{P_{\alpha,\beta}^n\}$  ( $\alpha, \beta \in \{0,1,2\}$ ), where  $\alpha$  specifies the number of *directions* in which the cell spills grains (within its own sheet), and  $\beta$  is the number of spill directions on the other sheet. For instance,  $P_{2,1}^n$  is the probability that a cell spills both upwards and to the right on its own sheet, and either up or to the right on the other sheet. If  $\alpha=1$  (or  $\beta=1$ ) then the direction of the spill (up or right) is chosen at random. For example, in our original two-sheet model, only spills of the types  $P_{0,0}^0$ ,  $P_{2,0}^0$ , and  $P_{2,2}^0$  can occur. [This characterization of a cell's dynamics is not quite complete. It is also necessary to distinguish between two subcases of  $P_{1,1}^n$ , namely, the case when the spills on sheets A and B are in the same direction (i.e., both to the right or both up), and when they are not (i.e., one to the right and one up). We shall denote these symmetric and antisymmetric subcases as  $P_{1,1,s}^n$ ,  $P_{1,1,a}^n$ , respectively ( $P_{1,1,s}^n + P_{1,1,a}^n = P_{1,1}^n$ ).]

The next step is to course grain the cells again (into  $2^{n+1} \times 2^{n+1}$  blocks), and construct the corresponding evolution rules governing the new, enlarged cells. In other words, we wish to determine the RG map that relates  $P^n$  to  $P^{n+1}$ . To do so, we utilize the procedure developed in Ref. [10] for the case of a single-sheet automaton model. This method involves considering two-by-two blocks of the smaller ( $2^n \times 2^n$ ) cells, and going through all possible combinatoric possibilities to derive the probabilities for the enlarged cells. We refer the reader to Ref. [10] for a description of this basic method. There is, however, one critical departure that we make from the procedure cited in Ref. [10]. Namely, construction of the RG map for the single automaton case in Ref. [10] proved arduous but analytically tractable (the RG map contained on the order of 100 terms). However, for our case of two weakly interacting automaton, the resulting RG map is much more complex (it contains several orders of magnitude more terms!), rendering its explicit calculation infeasible. As described below, to surmount this difficulty we use Monte Carlo simulations to numerically sample the various combinatoric possibilities associated with  $P^n$ , and in this manner can approximate the probability matrix of the enlarged cells  $P^{n+1}$ . We then repeat this procedure and look at the limiting behavior of the resulting sequence of probability matrices.

Specifically, the renormalization mapping is computed as follows. Assume that the evolution matrix  $P^n$ , which describes the dynamics of cells of size  $2^n \times 2^n$ , is known. We now consider enlarged cells of size  $2^{n+1} \times 2^{n+1}$ , formed by grouping together four ( $2^n \times 2^n$ ) cells into  $2 \times 2$  blocks. The rules governing the behavior of these enlarged cells are obtained in the following manner. Imagine dropping a single grain onto the lower-left subcell of a ( $2 \times 2$ ) enlarged cell. For sake of argument assume this cell lies on the top sheet (sheet A). The subcell will respond according to rules defined by the evolution matrix  $P^n$ . For example, the probability of that subcell not toppling is given by  $P_{0,0}^n$ , while the probability of that subcell toppling onto all four of its downstream neighbors (two on each sheet) is given by  $P_{2,2}^n$ . We continue to follow the avalanching process until all subcells

(in both the cell on sheet A and the corresponding cell on sheet B) are quiescent. We now check where grains have exited the large cell. For example, if grains are spilled to the right on sheet A and to the right and up on sheet B, then we have an event of type (1,2). Thus we only count the number of directions in which grains exit the large cell, not the total number grains in each direction, for this part of the analysis. We then repeat this procedure a large number of times. (Typically about  $10^6$  trials are necessary for adequate accuracy.) At the end of this procedure we have a unnormalized matrix of evolution numbers  $\Lambda_{\alpha,\beta}$  which is the total number of type ( $\alpha,\beta$ ) events which occurred. However, as discussed in Refs. [8] and [10], we need to “normalize” these probabilities in a specific manner. In order to do this we compute  $\Lambda_{0,0}$  differently than the other elements of the matrix  $\Lambda$ . The procedure we use is that for each sample we take (i.e., for each drop onto the initial subcell), we count the total number of grains that exit the large cell. If this number is larger than zero we add one less than this number to  $\Lambda_{0,0}$ . This “normalization” is very similar to the one used by Hasty and Wiesenfeld but slightly easier to compute in simulations (but would be more difficult analytically), and also easier to generalize for more complex sandpiles (such as ones in higher dimensions). In fact, when applied to the single sheet model studied by Hasty and Wiesenfeld, it leads to slightly more accurate estimates of the critical exponent than their procedure does. (In the single-sheet model, the difference between the two procedures arises when an upper-right subcell spills two grains in the same direction out of the large cell. In this case our procedure adds one more to  $\Lambda_{0,0}$  than Hasty and Wiesenfeld's would.)

Given the matrix  $\Lambda$  it is straightforward to compute  $P^{n+1}$ . Let  $|\Lambda|$  be the sum of all the elements of  $\Lambda$ . We view the elements as probability amplitudes and thus we need to convert them into true probabilities to continue the renormalization procedure, thus  $P_{\alpha,\beta}^{n+1} = \Lambda_{\alpha,\beta} / |\Lambda|$ .

Representative results for the renormalization process are as follows (accurate to about  $\pm 0.002$ ):

$$P^0 = \begin{pmatrix} 0.500 & 0.000 & 0.000 \\ 0.000 & 0.000 & 0.000 \\ 0.475 & 0.000 & 0.025 \end{pmatrix},$$

$$P^4 = \begin{pmatrix} 0.583 & 0.067 & 0.011 \\ 0.088 & 0.105 & 0.034 \\ 0.014 & 0.038 & 0.055 \end{pmatrix},$$

$$P^{16} = \begin{pmatrix} 0.700 & 0.001 & 0.000 \\ 0.001 & 0.185 & 0.001 \\ 0.000 & 0.001 & 0.112 \end{pmatrix},$$

$$P^\infty = \begin{pmatrix} 0.702 & 0.000 & 0.000 \\ 0.000 & 0.185 & 0.000 \\ 0.000 & 0.000 & 0.113 \end{pmatrix}.$$

This has three immediate consequences:

(i) Having set the initial probability matrix  $P^0$  to correspond with our original two-sheet model with weak coupling ( $\rho=0.05$ ), we find that the RG map quickly converges to the limiting probability matrix  $P^\infty$ . The principal result here is that this limiting matrix is diagonal. This shows that in any large avalanche (i.e., on large spatial scales) the number of topplings on the top sheet and bottom sheet will be approximately equal, thereby establishing the emergence of LSS in this model.

(ii) If we instead vary the values of the starting probability matrix  $P^0$  (corresponding to the generalized two-sheet models), we find that all (nontrivial) choices of starting configurations  $P^0$  display the *same* limiting behavior  $P^\infty$  in the renormalization analysis. Hence these generalized models fall into the same universality class as the original, and therefore will all exhibit the same behavior (LSS) on large spatial scales. In particular, this shows, for example, that our original two-sheet model with weak coupling ( $\rho=0.05\ll 1$ ) is in the same universality class as a two-sheet model with full coupling ( $\rho=1$ ). In other words, when viewed on larger and larger spatial scales, the weakly interacting automata begin to act as though they were very strongly coupled. This strengthening of effective coupling constant with length scale can be regarded as the source of the high level of correlation between the two systems.

(iii) If we examine the intermediate stages of the transition process  $P^0 \rightarrow P^1 \rightarrow \dots \rightarrow P^\infty$ , an interesting feature appears: Under the RG map a general starting matrix  $P^0$  will first become approximately symmetric (e.g.,  $P^4$ ) prior to becoming nearly diagonal (e.g.,  $P^{16}$ ). (In the symmetric phase,  $P_{\alpha\beta}^n \approx P_{\beta\alpha}^n$ , and  $P_{11a}^n \approx 0$ .) Hence the renormalization analysis leads to a prediction that, in our original two-sheet automaton model, adding a grain to a site on, say, sheet A, has an equal likelihood of inducing an (intermediate-size) avalanche on sheet B as on sheet A, even though the local dynamics dictate that small avalanches are much more likely to occur on the sheet to which the additional grain was added than on the other sheet. This is surprising in that we started with a model in which the coupling between neighboring lattice sites was highly asymmetric [in the sense that each site is strongly coupled with its neighbors on its same sheet but only weakly coupled with its neighbors on the other sheet (i.e.,  $\rho=0.05$ )], and yet we are led to the conclusion that on larger length scales the effective inter-sheet coupling becomes equal in strength to the intrasheet coupling. A type of large-scale ‘‘coupling symmetry’’ has thus emerged. This prediction was tested and borne out by numerical simulations of the automaton, as illustrated (by the dashed line) in Fig. 3.

We can gain further insight into the nature of this statistical synchrony and, in particular, the onset of this coupling symmetry, by forgoing the above renormalization approach and instead utilizing an algebraic argument based on work by Dhar [13] for an analogous model (see also Zhang [14]). We will take our original two-sheet model and calculate the two-point correlation function  $C(x,y)$ , which describes the expected number of topplings at site  $y$ , due to the avalanche caused by adding a single grain to lattice site  $x$ . What we will prove is that if two sites  $x$  and  $y$  are sufficiently far apart, then a symmetry in the correlation function  $C(x,y)$

$\approx C(x,\bar{y})$  develops, where  $\bar{y}$  denotes the site corresponding to  $y$  but on the opposite sheet. This calculation will show that adding a grain to a given site on one sheet will induce the *same* expected number of topplings on some distant site on its own sheet as it will on the corresponding (distant) site on the other sheet—despite the weakness of the coupling between the two sheets. (In what follows, it will be convenient to let  $x_L, x_B$  denote the the neighboring sites immediately to the left or below a site  $x$ , on the same sheet.)

First, define a toppling matrix  $-\Delta(x,y)$ , which specifies the average number of grains that will spill directly from a site  $x$  to site  $y$  in the event that  $x$  topples. (Note that here we count only *direct* spillage between the two sites, not grains that might spill from  $x$  to  $y$  by way of intermediate sites.) For our original two-sheet model, we have  $-\Delta(y,y) = -2(1+\rho)$ ;  $-\Delta(y_L,y) = 1$ ;  $-\Delta(y_B,y) = 1$ ;  $-\Delta(\bar{y}_L,y) = \rho$ ;  $-\Delta(\bar{y}_B,y) = \rho$ . All other components of  $\Delta(x,y)$  are zero. As in Dhar [13], it is straightforward to show that the toppling matrix and correlation function obey the following general relation:  $\sum_z C(x,z)\Delta(z,y) = \delta_{x,y}$ . For our model, the only terms in the toppling matrix which contribute to the summation are the four neighboring sites of  $y$ . Thus the relationship reduces to  $C(x,y_L) + C(x,y_B) + \rho C(x,\bar{y}_L) + \rho C(x,\bar{y}_B) = 2(1+\rho)C(x,y)$ . We observe, however, that this relation is precisely the formula for the probability that a certain random walk starting at site  $x$  will hit site  $y$ . In this random walk, at every step the walker is equally likely to go up or right, and switches between sheets with probability  $\rho/(1+\rho)$ . It follows then that the probability that a walker starting on one sheet will end up on that same sheet  $k$  steps later is  $(1 + [(1-\rho)/(1+\rho)]^k)/2$ . Since this approaches  $1/2$  for large  $k$ , we conclude that  $C(x;y) \approx C(x;\bar{y})$  for  $x$  and  $y$  sufficiently far apart. (More precisely, the fractional difference between these correlations scales like  $[(1-\rho)/(1+\rho)]^k$ , where  $k$  is the distance between sites  $x$  and  $y$  in the ‘‘taxicab’’ metric, assuming of course that  $y$  is reachable from  $x$ , else both correlations are 0. Note here that the ‘‘taxicab’’ metric is defined by the minimum number of steps separating two points on a lattice.) Hence this demonstrates that on sufficiently large spatial scales, the intrasheet and intersheet coupling become equal.

#### IV. CONCLUSIONS

In summary, we have examined (in the context of a few specific examples) the nature of the complex correlations arising between weakly interacting automata, and have used a Monte Carlo implementation of a renormalization-group analysis to understand the appearance of large-scale statistical synchrony in these systems. Since both our methods of analysis and the properties of SOC systems are extremely robust (e.g., the extension of the algebraic analysis to more general models is straightforward), we believe that the types of intersandpile correlations found here will likely be a generic feature of other weakly coupled SOC systems. In fact, preliminary analysis suggests that these properties even arise in some automata models which do not exhibit SOC, such as dissipative models. We note that our Monte Carlo approach

for studying the RG map turns out to be remarkably efficient and may in fact provide the key to applying renormalization to more complex automaton models.

Last, we remark that the emergence of strong statistical correlations described here raises a number of interesting questions, including (i) is there some universal scaling law describing how the length scale at which strong correlations arise varies with the intersheet coupling strength; and (ii)

might it be possible to recast this phenomenon as a type of phase transition that occurs with increasing spatial scale?

#### ACKNOWLEDGMENT

We would like to thank D. Dhar for helpful comments on the manuscript.

- 
- [1] M. Rosenblum, A.S. Pikovsky, and J. Kurths, *Phys. Rev. Lett.* **76**, 1804 (1996); **78**, 4193 (1997).
- [2] L. Kocarev and U. Parlitz, *Phys. Rev. Lett.* **76**, 1816 (1996).
- [3] N.F. Rulkov, M.M. Sushchik, L.S. Tsimring, and H.D.I. Abarbanel, *Phys. Rev. E* **51**, 980 (1995).
- [4] L.M. Pecora and T.L. Carroll, *Phys. Rev. Lett.* **64**, 821 (1990).
- [5] P. Bak, C. Tang, and K. Wiesenfeld, *Phys. Rev. Lett.* **59**, 381 (1987); *Phys. Rev. A* **38**, 364 (1988).
- [6] P. Bak and K. Chen, *Physica D* **38**, 5 (1984); K. Chen and P. Bak, *Phys. Lett. A* **140**, 299 (1989); Z. Olami, H.J.S. Feder, and K. Christensen, *Phys. Rev. Lett.* **68**, 1244 (1992); V.M. Vinokur, M.V. Feigelman, and V.B. Geshkenbein, *ibid.* **67**, 915 (1991); P. Bak and K. Sneppen, *ibid.* **71**, 4083 (1993).
- [7] We note that P. Krugman [in *The Self-Organizing Economy* (Blackwell Publishers, Cambridge, MA, 1996)] has suggested, but not formally analyzed, coupled sandpiles as a model of international trade.
- [8] L. Pietronero, A. Vespignani, and S. Zapperi, *Phys. Rev. Lett.* **72**, 1690 (1994).
- [9] A. Vespignani, S. Zapperi, and L. Pietronero, *Phys. Rev. E* **51**, 1711 (1995).
- [10] J. Hasty and K. Wiesenfeld, *Phys. Rev. Lett.* **81**, 1722 (1998).
- [11] D. Dhar and R. Ramaswamy, *Phys. Rev. Lett.* **63**, 1659 (1989).
- [12] We note that these models are in a different universality class than the related models described in R. Pastor-Satorras and A. Vespignani, *J. Phys. A* **33**, L33 (2000).
- [13] D. Dhar, *Phys. Rev. Lett.* **64**, 1613 (1990).
- [14] Y.C. Zhang, *Phys. Rev. Lett.* **63**, 470 (1989).